Structure Assignment, Electronic Properties, and Magnetism Quenching of Endohedrally Doped Neutral Silicon Clusters, SinCo (n=10−12)

ARTICLE *in* THE JOURNAL OF PHYSICAL CHEMISTRY A · APRIL 2014

Impact Factor: 2.69 · DOI: 10.1021/jp500928t · Source: PubMed

10 AUTHORS, INCLUDING:

Jonathan T Lyon
Clayton State University
44 PUBLICATIONS **1,024** CITATIONS
SEE PROFILE

André Fielicke
Technische Universität Berlin
101 PUBLICATIONS **2,401** CITATIONS
SEE PROFILE

Ewald Janssens
University of Leuven
94 PUBLICATIONS **1,762** CITATIONS
SEE PROFILE

THE JOURNAL OF PHYSICAL CHEMISTRY A

Article

pubs.acs.org/JPCA

Structure Assignment, Electronic Properties, and Magnetism Quenching of Endohedrally Doped Neutral Silicon Clusters, Si_nCo (n = 10−12)

Yejun Li,[†] Nguyen Minh Tam,[‡] Pieterjan Claes,[†,#] Alex P. Woodham,[§] Jonathan T. Lyon,[∥] Vu Thi Ngan,[‡,+] Minh Tho Nguyen,[‡] Peter Lievens,*[,†] André Fielicke,[§] and Ewald Janssens[†]

[†]Laboratory of Solid State Physics and Magnetism and [‡]Department of Chemistry, KU Leuven, 3001 Leuven, Belgium

[§]Institut für Optik und Atomare Physik, Technische Universität Berlin, 10623 Berlin, Germany

[∥]Department of Natural Sciences, Clayton State University, Morrow, Georgia 30260, United States

Supporting Information

ABSTRACT: The structures of neutral cobalt-doped silicon clusters have been assigned by a combined experimental and theoretical study. Size-selective infrared spectra of neutral Si_nCo (n = 10−12) clusters are measured using a tunable IR−UV two-color ionization scheme. The experimental infrared spectra are compared with calculated spectra of low-energy structures predicted at the B3P86 level of theory. It is shown that the Si_nCo (n = 10−12) clusters have endohedral caged structures, where the silicon frameworks prefer double-layered structures encapsulating the Co atom. Electronic structure analysis indicates that the clusters are stabilized by an ionic interaction between the Co dopant atom and the silicon cage due to the charge transfer from the silicon valence sp orbitals to the cobalt 3d orbitals. Strong hybridization between the Co dopant atom and the silicon host quenches the local magnetic moment on the encapsulated Co atom.

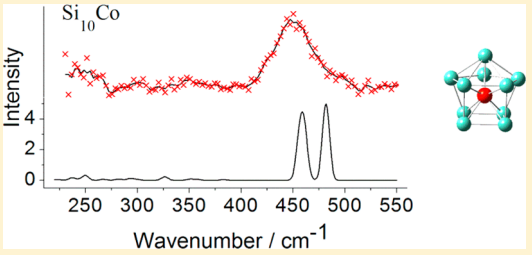

INTRODUCTION

The discovery of C_{60} has stimulated a vast amount of interest in caged molecules and atomic clusters because of their unique properties, which make them appealing candidates for building blocks of nanostructured materials.[1,2] The insertion of dopant atoms into hollow caged particles provides a valuable pathway to stabilize the cages and at the same time tailor their properties. The particular suitability of silicon clusters for applications related to the importance of silicon in the microelectronics industry stimulated a lot of research toward caged silicon clusters.[3−6] Contrary to the isolobal carbon, silicon favors sp^3 hybridization rather than sp^2 hybridization. Consequently, pure silicon clusters are reactive, and empty caged silicon structures are unstable, resulting in the formation of rather asymmetric silicon clusters. It was found that incorporating a single transition-metal atom may dramatically influence the structure and stability of the clusters. Examples are the hexagonal prism structure of $Si_{12}W$ and the Frank−Kasper polyhedrons $Si_{16}Ti$ and $Si_{16}V^+$.[3,4,6,7] It was also suggested that joining multiple endohedrally doped silicon clusters together in a row may lead to the formation of transition-metal-doped silicon nanorods.[8−10]

Several theoretical studies have indicated that strong hybridization between the dopant d orbitals and the silicon s and p orbitals strongly reduces or even quenches the local magnetic moment (LMM) of the impurity atom.[11−15] A recent DFT investigation has shown that the hydrogen termination of $Si_{20}Cr$, leading to $Si_{20}CrH_{20}$, saturates all Si dangling bonds and reduces the interaction between the Si_{20} cage and the central Cr dopant atom, thereby conserving the atomic LMM on the Cr atom.[16] These clusters are promising candidates for the realization of magnetic silicon nanoparticles, which have great potential for diverse applications in magnetic fluids, biotechnology, magnetic resonance, and data storage.[17]

Charged doped Si clusters have been intensively investigated via different experimental techniques, such as photoelectron spectroscopy,[18] photodissociation experiments,[19] and soft X-ray absorption spectroscopy.[20] Structural identification of cationic transition-metal-doped silicon clusters in the gas phase has been realized by infrared multiple photon dissociation (IR-MPD) spectroscopy in combination with DFT calculations.[3,21−23] In particular, it was shown that Si_nV^+ (n = 12−16)[3] and Si_nMn^+ (n = 12−14, 16)[21] clusters have caged structures. In those studies, the IR-MPD technique made use of messenger atom detachment as a marker for the resonant absorption of infrared photons by the clusters.[3,21−23] The inherent disadvantage of this technique is the possible perturbation of the cluster's structure by the adsorbed messenger atom, even though usually weakly bonded rare gas atoms are used as messengers.[24,25]

Special Issue: A. W. Castleman, Jr. Festschrift

Received: January 27, 2014
Revised: April 14, 2014

   dx.doi.org/10.1021/jp500928t | J. Phys. Chem. A XXXX, XXX, XXX−XXX

Experimental data for neutral transition-metal-doped silicon clusters is sparse because the complex formation of neutral silicon clusters with rare gas atoms is more difficult and ionization is required for mass spectrometric detection, which adds to the experimental complexity.[26] A valuable alternative to record the infrared absorption spectrum of gas-phase clusters relies on a two-color ionization scheme, where the absorption of a single or few IR photons prior to interaction with a UV photon lifts the total internal energy of the species above the ionization threshold. This tunable IR−UV two-color ionization (IR−UV2CI) technique has been successfully applied for the structural assignments of neutral Si_n (n = 6−10, 15),[27,28] Si_mC_n ($m + n$ = 6),[29] and $(MgO)_n$ (n = 3−16) clusters.[30] IR−UV2CI has the important advantages that it can be applied to neutral clusters and that there is no need for a messenger atom. Unfortunately, its applicability is limited by the (un)availability of tunable UV lasers with photon energies corresponding to the threshold ionization energies of the clusters.

In the current work, the IR−UV2CI spectra of neutral Si_nCo (n = 10−12) clusters are recorded, and their structures are assigned by comparison with results from DFT calculations. This work is the first experimental data about the structures of cobalt-doped silicon clusters. Moreover, it is the first structural assignment on neutral endohedrally doped silicon clusters. The structural, electronic, and magnetic properties of these clusters are investigated, and it is shown that there is a strong ionic interaction between the dopant Co atom and the silicon cage. Strong hybridization between the Co 3d orbitals and the silicon valence electron along with charge transfer from the silicon cage to Co atom quenches the LMM of the encapsulated Co atom.

EXPERIMENTAL AND THEORETICAL METHODS

The experiments are performed in a molecular beam setup[31] coupled to a beamline of the Free Electron Laser for Infrared eXperiments (FELIX) user facility at the FOM Institute for Plasma Physics, Nieuwegein, The Netherlands (recently moved to the Radboud University Nijmegen, The Netherlands).[32] The clusters are produced in a dual-target laser vaporization cluster source by pulsed ablation of cobalt and silicon plate targets (10 Hz, 532 nm, ∼20 mJ per pulse).[33] The Si_nCo clusters form by condensation of the vaporized material in a short pulse of He gas. Before expansion into the vacuum, the clusters are cooled in a thermalization channel that is attached to the source and held at a temperature of 115 K. The cluster beam is first skimmed and then shaped by an aperture with a 1 mm opening. Ions are removed from the beam by applying a voltage to the aperture, and the neutral clusters are ionized by an F_2 laser emitting 7.87 eV photons.

The ionized clusters are analyzed by a reflectron time-of-flight mass spectrometer. Species with vertical ionization energies (VIEs) close to (or slightly above) the photon energy of the ionization laser have a low intensity in the mass spectra (Figure 1a). In particular, the small signals recorded for Si_{10} and $Si_{10}Co$ could originate from hot fractions of the thermal cluster distribution, where the internal energy in combination with the UV photon energy is sufficient for ionization. The relative intensities of those species in the mass spectra changes if they are excited by the absorption of one or more IR photons prior to interaction with the UV radiation (Figure 1b and c). Indeed, resonant absorption of the IR light increases the internal energy of a cluster and enhances the ionization efficiency,[30] which is reflected by an increase of the abundance of the corresponding

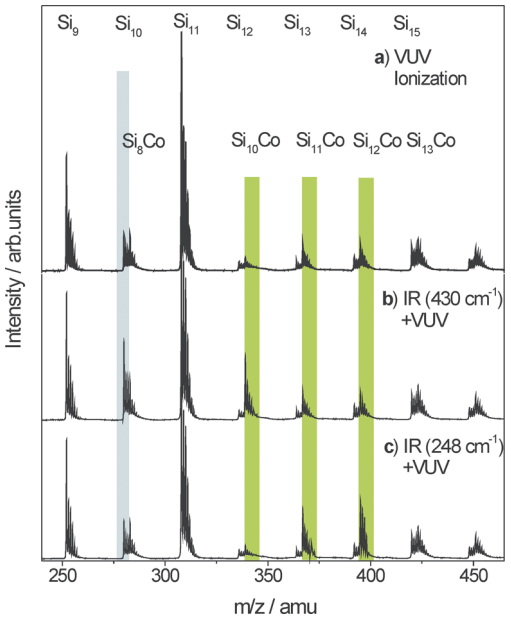

Figure 1. Mass spectra of neutral Si_n (n = 9−16) and Si_nCo (n = 7−14) clusters obtained under different ionization conditions. (a) Mass spectrum obtained by ionization with 7.87 eV UV photons solely. (b) Prior irradiation of the neutral cluster distribution with intense IR light at 430 cm^{-1} significantly increases the signal of Si_{10} and $Si_{10}Co$, while the remaining mass spectrum is nearly unchanged. (c) Irradiation with IR light of 248 cm^{-1} followed by UV ionization enhances the intensities of $Si_{11}Co$ and $Si_{12}Co$.

cluster ion in the mass spectrum. To record the IR spectra, the intense infrared laser beam delivered by FELIX is overlapped with the counter propagating molecular beam. The output of FELIX is tunable in the 40−2000 cm^{-1} range and consists of ∼5−8 μs long macropulses with a typical energy of ∼50 mJ. In the current experiment, FELIX was tuned over the 230−550 cm^{-1} range. Recording the signal enhancement, normalized for the laser fluence, yields the IR−UV2CI spectra of the neutral clusters.

Quantum chemical calculations were performed using the Gaussian 09 program package.[34] The B3P86 functional is employed in combination with the 6-311+G(d) basis sets, which was shown to be successful for the structural assignment of cationic manganese-doped silicon clusters without the need for a scaling factor.[21] The searches for energy minima are conducted using different approaches. At first, the generation of candidate structures for each Si_nCo cluster system is initially based on the structures previously reported in the literature.[11,12,15] In the second approach, we use a stochastic genetic algorithm to more comprehensively probe the configurational space.[35] The equilibrium structures that are initially detected using the hybrid B3LYP functional together with the 6-31G basis set are reoptimized using the B3P86 functional with the larger 6-311+G(d) basis set. In addition, initial structures of clusters Si_nCo are manually constructed by either substituting one Si atom of the Si_{n+1} framework by one Co atom or adding the Co atom at various positions on surfaces of the Si_n clusters. For each structural isomer, different spin multiplicities equal to $2S + 1$ = 2, 4, and 6 have been considered. Frequency calculations are performed within the harmonic approximation using analytical second derivatives. The calculated infrared spectra are folded with a Gaussian line width function of 8 cm^{-1} full width at half-maximum. Magnetic moments, atomic

dx.doi.org/10.1021/jp500928t | J. Phys. Chem. A XXXX, XXX, XXX−XXX

charges, and electronic configurations are evaluated based on natural population analysis, which is performed at the same level of theory using the NBO 5.9 program.[36] Partial densities of states (PDOSs) are discussed on the basis of Mulliken population analysis, which gives good results for the valence electrons but is less reliable for the unoccupied levels.

STRUCTURAL ASSIGNMENT OF Si_NCo (N = 10−12)

Figure 2 shows the experimental IR−UV2CI spectra of Si_nCo (n = 10−12). Of the produced Si_nCo clusters, only for n = 10−12 IR−UV2CI spectra could be recorded (see the Supporting Information (SI)). This likely implies that only for n = 10−12 is the ionization energy of the clusters close to 7.87 eV. The calculated IR spectra of the predicted lowest-energy isomers are also shown in Figure 2. Additional low-lying isomers are shown if they also show reasonable agreement with the experimental spectra, and therefore, their presence in the molecular beam cannot be excluded. All assigned isomers have a doublet state, while the higher spin states, that is, quartet and sextet, are typically at least 0.2 eV higher in energy. A detailed comparison of the experimental spectra with computed spectra of various low-energy isomers is presented in the SI.

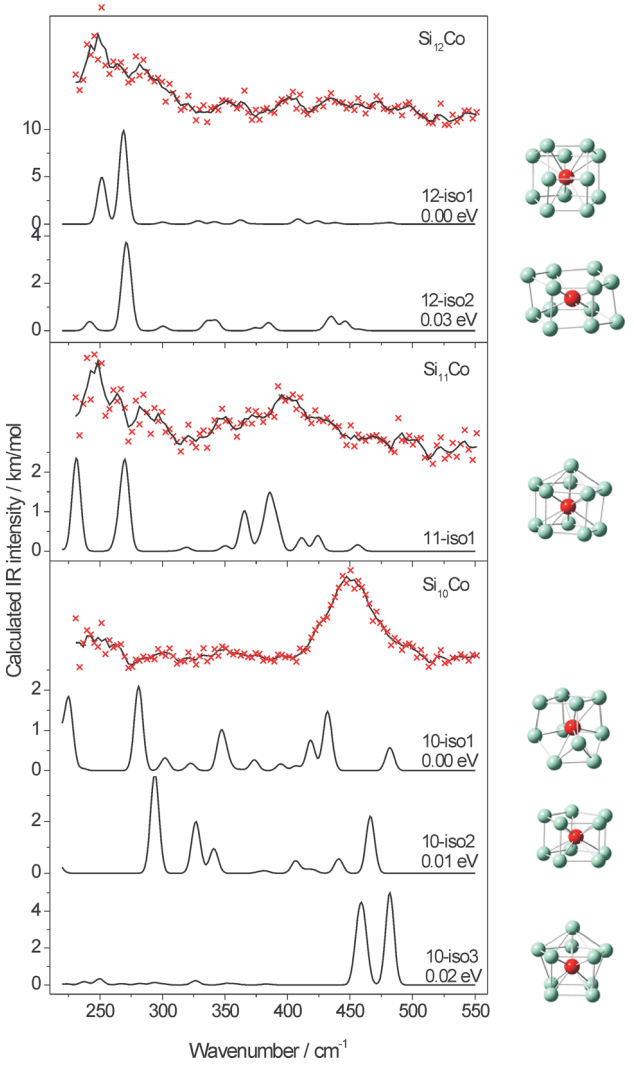

Figure 2. Comparison of the experimental IR−UV2CI spectra (upper traces) of Si_nCo (n = 10−12) and the corresponding calculated infrared spectra for the obtained lowest-energy isomers and additional low-energy isomers that fit the experiment well (lower traces). The geometries of these isomers are shown on the right. The red crosses are the original data points, while the full lines correspond to a three-point running average.

The signal-to-noise ratio of the IR−UV2CI spectra depends on the ionization energy of the clusters. Calculated VIEs of the assigned isomers (see below) of Si_nCo (n = 10−12) are listed in Table 1. The calculated VIE of $Si_{10}Co$ (8.28 eV) is higher than the photon energy of the ionization laser light (7.87 eV), while $Si_{11}Co$ and $Si_{12}Co$ have lower values (7.44 and 7.21 eV, respectively). Without prior IR excitation, the ionization efficiency of a single 7.87 eV photon is low for $Si_{10}Co$, while it is nonzero for $Si_{11}Co$ and $Si_{12}Co$, as is evidenced by their corresponding intensities in Figure 1a. In the two-color ionization process, the IR excitation strongly enhances the ionization efficiency of $Si_{10}Co$, explaining the better signal-to-noise ratio of its IR−UV2CI spectrum compared to those of $Si_{11}Co$ and $Si_{12}Co$. It should be noted, however, that in the previous studies, the IR−UV2CI spectra could only be obtained for species with ionization energies in a narrow range of about 0.2 eV around the UV photon energy,[27−30] which indicates that either the threshold ionization efficiency curve of Si_nCo (n = 10−12) is shallow around 7.87 eV or that the present level of theory (B3P86/6-311+G(d)) gives significant uncertainties when predicting the ionization energies.

The IR−UV2CI of $Si_{10}Co$ is characterized by one intense and broad band between 410 and 490 cm^{-1} and additional less intense absorptions at around 245−270 cm^{-1}. These features are relatively well reproduced by **10-iso3**, a cage-like silicon structure encapsulating the Co atom. The Si framework has a double-layered structure, with a rhombus and pentagonal layer and one additional Si atom on the top of the pentagon. The **10-iso3** has three intense bands centered at 456, 460, and 480 cm^{-1} and several small bands at around 237 and 250 cm^{-1}, explaining the experimental features. The structure of **10-iso1** also has a rhombus and pentagon layer, with one additional Si atom bridging an edge of the pentagon and a corner of the rhombus, while **10-iso2** is a pentagonal prism. Earlier studies have predicted **10-iso3** (ref 12) and **10-iso2** (ref 11) as the lowest-energy structures of $Si_{10}Co$. In the current work, **10-iso3** is only 0.02 and 0.01 eV higher in energy than **10-iso1** and **10-iso2**, respectively; these energy differences are well below the computational accuracy. The infrared spectra of **10-iso1** and **10-iso2** do not match with the experiment, and their existence can be excluded. The **10-iso3** is therefore assigned as the isomer of $Si_{10}Co$ that is present in the experiment.

The IR−UV2CI spectrum of $Si_{11}Co$ has intense features between 230 and 300 cm^{-1} with bands at 245, 263, and 283 cm^{-1} and less intense features between 340 and 440 cm^{-1}. The IR spectrum of the calculated lowest-energy isomer of $Si_{11}Co$, **11-iso1**, explains the experiment reasonably. It has two intense absorption bands centered at 230 and 270 cm^{-1} and several less intense bands at 350, 366, 385, 412, and 423 cm^{-1}, consistent with the experimental features, though the calculated band at 270 cm^{-1} seems to be split and less intense in the experiment. The **11-iso1** has a caged structure that is composed of a pentagonal prism, encapsulating the Co atom, with a Si atom capping on one of the pentagonal faces. This isomer was earlier predicted as the ground-state structure of $Si_{11}Co$.[11,12]

The experimental IR spectrum of $Si_{12}Co$ agrees quite well with the IR spectrum of the lowest-energy isomer, **12-iso1**, which is dominated by two intense absorption bands centered

dx.doi.org/10.1021/jp500928t | J. Phys. Chem. A XXXX, XXX, XXX−XXX

Table 1. VIE, Singly Occupied Molecular Orbital (SOMO) (α)−Lowest Unoccupied Molecular Orbital (LUMO) (β) Gap, Atomic Charge on Co, Natural Electronic Configuration (NEC), and LMM of the Co Atom in the Assigned Isomers of Si_nCo (n = 10−12)

n	VIE (eV)	SOMO−LUMO (eV)	charge (eV)	NEC	LMM (μ_B)
10-iso3	8.28	2.352	−1.514	$3d^{9.35}4s^{0.45}4p^{0.33}4d^{0.35}5s^{0.03}$	0.53
11-iso1	7.44	1.189	−1.382	$3d^{9.50}4s^{0.38}4p^{0.25}4d^{0.20}5s^{0.05}$	0.08
12-iso1	7.21	1.153	−1.046	$3d^{9.36}4s^{0.36}4p^{0.17}4d^{0.11}5s^{0.05}$	0.13

at 250 and 268 cm^{-1}. The presence of **12-iso2** (+0.03 eV) can, however, not be ruled out. This isomer has one intense band (270 cm^{-1}) in the wavelength range investigated. Both **12-iso1** and **12-iso2** have endohedral structures. The **12-iso1** is a bicapped and distorted pentagonal prism and was predicted as the ground state of $Si_{12}Co$ in ref 11, while **12-iso2** is a distorted hexagonal prism, which was the lowest-energy isomer found in ref 37.

We conclude that the structures of Si_nCo (n = 10−12) are endohedral cages. Earlier mass spectrometric experiments, in which Ar physisorption was used as a structural probe, already indicated that the Co dopant atom in cationic Si_nCo^+ clusters is encapsulated from n = 8 onward.[9] This earlier experiment could, however, not provide detailed structural information.

RESULTS AND DISCUSSION

The gap between the singly occupied molecular orbital (SOMO) and the lowest unoccupied molecular orbital (LUMO), the atomic charges on the Co atoms, the natural electronic configuration (NEC), and the LMM of the Co atoms in Si_nCo (n = 10−12) are listed in Table 1. The SOMO of the clusters has spin-up character, while the LUMO is of spin-down type. Despite the similar electronegativity of Si and Co, the Co atom acts as an electron acceptor, and an ionic interaction between the dopant Co atom and Si cage occurs. All clusters show a significant charge transfer of about 1−1.5 e from the Si cages to the encapsulated Co dopant atoms. The multicenter bonding character associated with the Co atom may also benefit from the small radius of the Co atom.[38] These combined effects stabilize the Si_n cage. In particular, $Si_{10}Co$ is electronically stabilized, as is reflected by a relatively high SOMO−LUMO gap. The NEC indicates that, while there is mainly electron transfer from the Si cage to the Co 3d orbitals, there is also rearrangement among the 3d, 4s, and 4p orbitals of the Co atom itself.

The electronic density of states (DOS) of $Si_{10}Co$ is plotted in Figure 3 together with the PDOS projection on Si and Co s, p, and d atomic orbitals (AOs). The PDOS is derived using Mulliken population analysis and gives good results for the valence electrons but is less reliable for the unoccupied levels. The DOS and PDOS of $Si_{11}Co$ and $Si_{12}Co$ are given in the SI. The DOS illustrates the presence of an electronic shell structure in $Si_{10}Co$. The shapes of the molecular orbitals (MOs) can be compared with the wave functions of a free electron in a spherically symmetric potential. In its simplest version, the phenomenological shell model assumes that the valence electrons of a cluster are delocalized over the whole cluster, where the nuclei and core electrons act as a simple mean-field potential. Accordingly, the MOs have shapes similar to those of the s, p, d, ... AOs. Therefore, the MOs are labeled hereafter by capital S, P, D, ... letters. Each electronic shell $(NL)^x$ is characterized by a radial quantum number N (N = 1, 2, 3, ...) and an angular quantum number L (L = S, P, D, ...). Enhanced stability is expected if the number of delocalized

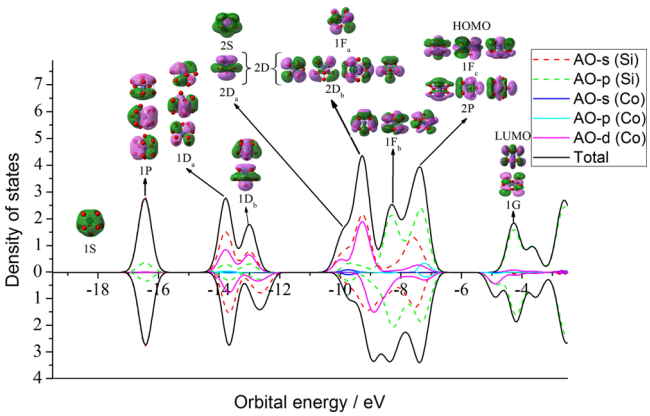

Figure 3. Calculated total DOS (black line) and PDOS (other lines) for the spin-up (positive DOS) and spin-down (negative DOS) states of the assigned isomer of $Si_{10}Co$. The shapes of the MOs are also shown and are labeled using the convention discussed in the text.

electrons corresponds to a closed electronic structure, that is, filled shells of electrons. The sequence of the electronic shells depends on the shape of the confining potential.[39] For a spherical cluster with a square well potential, the orbital sequence is $(1S)^2(1P)^6(1D)^{10}(2S)^2(1F)^{14}(2P)^6(1G)^{18}(2D)^{10}(1H)^{22}$..., corresponding to shell closure at 2, 8, 18, 20, 34, 40, 58, 68, 90, ... itinerant electrons.[40] There are 49 valence electrons in $Si_{10}Co$ (4 for each Si atom and 9 for Co). By comparison of the wave functions, the level sequence of the occupied electronic states in $Si_{10}Co$ can be described as $(1S)^2(1P)^6(1D_a)^6(1D_b)^4(2S)^2(2D_a)^2(1F_a)^2(2D_b)^8(1F_b)^6(1F_c)^6(2P)^5$. The subscripts a, b, and c indicate that the degeneracy of the high angular momentum states (1D, 2D, and 1F) is lifted because of crystal field splitting related to the nonspherical symmetry of the cluster. The most important difference with the energy level sequence of free electrons in a square well potential is the lowering of the 2D level. Examination of the 2D MOs shows that they are mainly composed of the Co 3d AOs, representing the strong hybridization between the central Co atom and the surrounding Si cage.

The strong hybridization of the Co 3d electrons with the Si valence electrons (evidenced by the PDOS shown in Figure 3) has implications for the magnetic moment of the central dopant atom. According to Hund's rule, the atomic magnetic moment of the Co atom ([Ar] $3d^74s^2$) is 3 μ_B, while the LMM of the Co atom in these Si_nCo clusters is quite small and almost quenched, as shown in Table 1. This result is also consistent with earlier theoretical studies.[11,12,15] The quenched magnetic moment can be attributed to the charge transfer and the strong hybridization between the Co 3d orbitals and Si 3s, 3p orbitals.

CONCLUSIONS

In summary, we have investigated the structures of neutral Si_nCo (n = 10−12) clusters by a combination of experimental infrared spectra, recorded using the tunable IR−UV2CI

dx.doi.org/10.1021/jp500928t | J. Phys. Chem. A XXXX, XXX, XXX−XXX

technique, and DFT predictions at the B3P86/6-311+G(d) level of theory. It is shown that the Si_nCo (n = 10−12) clusters form endohedral caged structures where the silicon framework prefers a double-layered structure. The caged structures are stabilized by a strong ionic interaction between the encapsulated Co dopant atom and the silicon cage due to the charge transfer from Si to Co. The DOS reveals a clear electronic shell structure, and there is a strong interaction between the Co 3d orbitals and the silicon sp valence electrons. Because of charge transfer, the Co 3d orbitals are formally filled, and its magnetic moment is almost quenched.

■ ASSOCIATED CONTENT

Supporting Information

Mass spectrum and IR−UV2CI spectra of Si_nCo (n = 8−16) clusters, structures and calculated IR spectra of low energetic Si_nCo (n = 10−12) isomers, and density of states of the assigned isomers of $Si_{11}Co$ and $Si_{12}Co$. This material is available free of charge via the Internet at http://pubs.acs.org.

■ AUTHOR INFORMATION

Corresponding Author

*E-mail: peter.lievens@fys.kuleuven.be.

Present Addresses

#P.C.: Instituto de Física, Universidad Nacional Autónoma de México, México.

+V.T.N.: Faculty of Chemistry, Quy Nhon University, Vietnam.

Notes

The authors declare no competing financial interest.

■ ACKNOWLEDGMENTS

The authors gratefully acknowledge the support of the Stichting voor Fundamenteel Onderzoek der Materie (FOM) in providing beam time on FELIX and highly appreciate the skillful assistance of the FELIX staff. This work is supported by the European Community's FP7/2007-2013 (Grant No. 226716), the Research Foundation−Flanders (FWO), the KU Leuven Research Council (GOA program), and the Deutsche Forschungsgemeinschaft within FOR 1282 (FI 893/4-2). J.T.L. is grateful to the Alexander von Humboldt Foundation.

■ REFERENCES

(1) Moses, M. J.; Fettinger, J. C.; Eichhorn, B. W. Interpenetrating As_{20} Fullerene and Ni_{12} Icosahedra in the Onion-Skin $[As@Ni_{12}@As_{20}]^{3-}$ Ion. *Science* **2003**, *300*, 778−780.

(2) Castleman, A. W., Jr.; Khanna, S. N. Clusters, Superatoms, and Building Blocks of New Materials. *J. Phys. Chem. C* **2009**, *113*, 2664−2675.

(3) Claes, P.; Janssens, E.; Ngan, V. T.; Gruene, P.; Lyon, J. T.; Harding, D. J.; Fielicke, A.; Nguyen, M. T.; Lievens, P. Structural Identification of Caged Vanadium Doped Silicon Clusters. *Phys. Rev. Lett.* **2011**, *107*, 173401.

(4) Kumar, V.; Briere, T. M.; Kawazoe, Y. Ab Initio Calculations of Electronic Structures, Polarizabilities, Raman and Infrared Spectra, Optical Gaps, and Absorption Spectra of $M@Si_{16}$ (M = Ti and Zr) Clusters. *Phys. Rev. B* **2003**, *68*, 155412.

(5) Koyasu, K.; Akutsu, M.; Mitsui, M.; Nakajima, A. Selective Formation of MSi_{16} (M = Sc, Ti, and V). *J. Am. Chem. Soc.* **2005**, *127*, 4998−4999.

(6) Hiura, H.; Miyazaki, T.; Kanayama, T. Formation of Metal-Encapsulating Si Cage Clusters. *Phys. Rev. Lett.* **2001**, *86*, 1733−1736.

(7) Reveles, J. U.; Khanna, S. N. Electronic Counting Rules for the Stability of Metal−Silicon Clusters. *Phys. Rev. B* **2006**, *74*, 035435.

(8) Singh, A. K.; Briere, T. M.; Kumar, V.; Kawazoe, Y. Magnetism in Transition Metal Doped Silicon Nanotubes. *Phys. Rev. Lett.* **2003**, *91*, 146802.

(9) Janssens, E.; Gruene, P.; Meijer, G.; Wöste, L.; Lievens, P.; Fielicke, A. Argon Physisorption as Structural Probe for Endohedrally Doped Silicon Clusters. *Phys. Rev. Lett.* **2007**, *99*, 063401.

(10) Menon, M.; Andriotis, A. N.; Froudakis, G. E. Structure and Stability of Ni-Encapsulated Si Nanotube. *Nano Lett.* **2002**, *2*, 301−304.

(11) Wang, J.; Zhao, J.; Ma, L.; Wang, B.; Wang, G. H. Structure and Magnetic Properties of Cobalt Doped Si_n (n = 2−14) Clusters. *Phys. Lett. A* **2007**, *367*, 335−344.

(12) Ma, L.; Zhao, J.; Wang, J. G.; Lu, Q. L.; Zhu, L. Z.; Wang, G. H. Structure and Electronic Properties of Cobalt Atoms Encapsulated in Si_n (n = 1−13) Clusters. *Chem. Phys. Lett.* **2005**, *411*, 279−284.

(13) Zamudio-Bayer, V.; Leppert, L.; Hirsch, K.; Langenberg, A.; Rittmann, J.; Kossick, M.; Vogel, M.; Richter, R.; Terasaki, A.; Möller, T.; von Issendorff, B.; Kümmel, S.; Lau, J. T. Coordination-Driven Magnetic-to-Nonmagnetic Transition in Manganese-Doped Silicon Clusters. *Phys. Rev. B* **2013**, *88*, 115425.

(14) Khanna, S. N.; Rao, B. K.; Jena, P. Magic Numbers in Metallo−Inorganic Clusters: Chromium Encapsulated in Silicon Cages. *Phys. Rev. Lett.* **2002**, *89*, 016803.

(15) Guo, L. J.; Zhao, G. F.; Gu, Y. Z.; Liu, X.; Zeng, Z. Density-Functional Investigation of Metal-Silicon Cage Clusters MSi_n (M = Sc, Ti, V, Cr, Mn, Fe, Co, Ni, Cu, Zn; n = 8−16). *Phys. Rev. B* **2008**, *77*, 195417.

(16) Palagin, D.; Reuter, K. $MSi_{20}H_{20}$ Aggregates: From Simple Building Blocks to Highly Magnetic Functionalized Materials. *ACS Nano* **2013**, *7*, 1763−1768.

(17) Lu, A. H.; Salabas, E. L.; Schuth, F. Magnetische Nanopartikel: Synthese, Stabilisierung, Funktionalisierung und Anwendung. *Angew. Chem.* **2007**, *119*, 1242−1266.

(18) Grubisic, A.; Ko, Y. J.; Wang, H.; Bowen, K. H. Photoelectron Spectroscopy of Lanthanide−Silicon Cluster Anions $LnSi_n^-$ ($3 \le n \le 13$; Ln = Ho, Gd, Pr, Sm, Eu, Yb): Prospect for Magnetic Silicon-Based Clusters. *J. Am. Chem. Soc.* **2009**, *131*, 10783−10790.

(19) Jaeger, J. B.; Jaeger, T. D.; Duncan, M. A. Photodissociation of Metal−Silicon Clusters: Encapsulated versus Surface-Bound Metal. *J. Phys. Chem. A* **2006**, *110*, 9310−9314.

(20) Lau, J. T.; Hirsch, K.; Klar, Ph.; Langenberg, A.; Lofink, F.; Richter, R.; Rittman, J.; Vogel, M.; Zamudio-Bayer, V.; Möller, T.; von Issendorff, B. X-ray Spectroscopy Reveals High Symmetry and Electronic Shell Structure of Transition-Metal-Doped Silicon Clusters. *Phys. Rev. A* **2009**, *79*, 053201.

(21) Ngan, V. T.; Janssens, E.; Claes, P.; Lyon, J. T.; Fielicke, A.; Nguyen, M. T.; Lievens, P. High Magnetic Moments in Manganese-Doped Silicon Clusters. *Chem.—Eur. J.* **2012**, *18*, 15788−15793.

(22) Ngan, V. T.; Gruene, P.; Claes, P.; Janssens, E.; Fielicke, A.; Nguyen, M. T.; Lievens, P. Disparate Effects of Cu and V on Structures of Exohedral Transition Metal-Doped Silicon Clusters: A Combined Far-Infrared Spectroscopic and Computational Study. *J. Am. Chem. Soc.* **2010**, *132*, 15589−15602.

(23) Gruene, P.; Fielicke, A.; Meijer, G.; Janssens, E.; Ngan, V. T.; Nguyen, M. T.; Lievens, P. Tuning the Geometric Structure by Doping Dilicon Clusters. *ChemPhysChem* **2008**, *9*, 703−706.

(24) Savoca, M.; Langer, J.; Harding, D. J.; Dopfer, O.; Fielicke, A. Incipient Chemical Bond Formation of Xe to a Cationic Silicon Cluster: Vibrational Spectroscopy and Structure of the Si_4Xe^+ Complex. *Chem. Phys. Lett.* **2013**, *557*, 49−52.

(25) Gehrke, R.; Gruene, P.; Fielicke, A.; Meijer, G.; Reuter, K. Nature of Ar Bonding to Small Co_n^+ Clusters and Its Effect on the Structure Determination by Far-Infrared Absorption Spectroscopy. *J. Chem. Phys.* **2009**, *130*, 034306.

(26) Claes, P.; Ngan, V. T.; Haertelt, M.; Lyon, J. T.; Fielicke, A.; Nguyen, M. T.; Lievens, P.; Janssens, E. The Structures of Neutral Transition Metal Doped Silicon Clusters, Si_nX (n = 6−9; X = V, Mn). *J. Chem. Phys.* **2013**, *138*, 194301.

(27) Fielicke, A.; Lyon, J. T.; Haertelt, M.; Meijer, G.; Claes, P.; de Haeck, J.; Lievens, P. Vibrational Spectroscopy of Neutral Silicon Clusters via Far-IR−VUV Two Color Ionization. *J. Chem. Phys.* **2009**, *131*, 171105.
(28) Haertelt, M.; Lyon, J. T.; Claes, P.; de Haeck, J.; Lievens, P.; Fielicke, A. Gas-Phase Structures of Neutral Silicon Clusters. *J. Chem. Phys.* **2012**, *136*, 064301.
(29) Savoca, M.; Lagutschenkov, A.; Langer, J.; Harding, D. J.; Fielicke, A.; Dopfer, O. Vibrational Spectra and Structures of Neutral Si_mC_n Clusters ($m + n = 6$): Sequential Doping of Silicon Clusters with Carbon Atoms. *J. Phys. Chem. A* **2013**, *117*, 1158−1163.
(30) Haertelt, M.; Fielicke, A.; Meijer, G.; Kwapien, K.; Sierka, M.; Sauer, J. Structure Determination of Neutral MgO Clusters — Hexagonal Nanotubes and Cages. *Phys. Chem. Chem. Phys.* **2012**, *14*, 2849−2856.
(31) Fielicke, A.; von Helden, G.; Meijer, G. Far-Infrared Spectroscopy of Isolated Transition Metal Clusters. *Eur. Phys. J. D* **2005**, *34*, 83−88.
(32) Oepts, D.; van der Meer, A. F. G.; van Amersfoort, P. W. The Free-Electron-Laser User Facility FELIX. *Infrared Phys. Technol.* **1995**, *36*, 297−308.
(33) Bouwen, W.; Thoen, P.; Vanhoutte, F.; Bouckaert, S.; Despa, F.; Weidele, H.; Silverans, R. E.; Lievens, P. Production of Bimetallic Clusters by a Dual-Target Dual-Laser Vaporization Source. *Rev. Sci. Instrum.* **2000**, *71*, 54−58.
(34) Frisch, M. J.; Trucks, G. W.; Schlegel, H. B.; Scuseria, G. E.; Robb, M. A.; Cheeseman, J. R.; Scalmani, G.; Barone, V.; Mennucci, B.; Petersson, G. A.; et al. *Gaussian 09*, revision D.01; Gaussian, Inc.: Wallingford, CT, 2013.
(35) Tai, T. B.; Nguyen, M. T. A Stochastic Search for the Structures of Small Germanium Clusters and Their Anions: Enhanced Stability by Spherical Aromaticity of the Ge_{10} and Ge_{12}^{2-} Systems. *J. Chem. Theory Comput.* **2011**, *7*, 1119−1130.
(36) Glendening, E. D.; et al. *NBO 5.9*; Theoretical Chemistry Institute, University of Wisconsin: Madison, WI, 2011; http://www.chem.wisc.edu/~nbo5.
(37) He, J.; Wu, K.; Sa, R.; Li, Q.; Wei, Y. (Hyper) Polarizabilities and Optical Absorption Spectra of MSi_{12} Clusters (M = Sc-Zn): A Theoretical Study. *Chem. Phys. Lett.* **2010**, *490*, 132−137.
(38) Avaltroni, F.; Steinmann, S. N.; Corminboeuf, C. How Are Small Endohedral Silicon Clusters Stabilized? *Phys. Chem. Chem. Phys.* **2012**, *14*, 14842−14849.
(39) Janssens, E.; Neukermans, S.; Lievens, P. Shells of Electrons in Metal Doped Simple Metal Clusters. *Curr. Opin. Solid State Mater. Sci.* **2004**, *8*, 185−193.
(40) de Heer, W. A. The Physics of Simple Metal Clusters: Experimental Aspects and Simple Models. *Rev. Mod. Phys.* **1993**, *64*, 611−676.